Fast computation and morphologic interpretation of the Adaptive Optics Point Spread Function

Venice 2001
Beyond
Conventional
Adaptive
Optics

Laurent Jolissaint and Jean-Pierre Veran

National Research Council of Canada, Herzberg Institute of Astrophysics
5071 West Saanich Road, Victoria, BC, V9E 2E7 CANADA

ABSTRACT

We reconsider here the computation of the long exposure AO PSF based on an analytical model of the spatial power spectrum of the residual phase (Rigaut et al. 1998). While this approach is not as accurate as others, it is much less demanding in terms of computations, and allows us to compute the AO PSF with a useful accuracy and within a reasonable time. It allows to compute AO corrected PSFs of giant telescopes within minutes, where other methods would take hours and days and would require parallel computations. We present a bi-dimensional formulation of the method, as well as an original interpretation of the wings of the AO PSF in term of the power spectrum of the residual phase. This leads to a very powerful tool to assess the effect of the different AO parameters on the different parts of the AO PSF. We present several examples of use of this tool and show that for giant telescopes (larger than 20 meters), the relationship between the residual phase spectrum and the PSF wings is much more critical than for a 4-10 meter class telescope, where these effects are hidden by the diffraction patterns.

1. INTRODUCTION

Several simulations tools have been developed to simulate the performance of adaptive optics system for the current telescopes. These methods rely on the computation of many instantaneous PSFs and/or the numerical computations of models that do not have any analytical solutions. These methods usually allow the user to set many different parameters and many different effects can be included, leading to very realistic simulations. The problem is that these methods require huge amounts of computation times and can not be scaled to the next generation of giant telescopes ($D \geq 20m$) without requiring state of the art parallel computers. This complexity is related to the size of the arrays involved in the simulation, to represent the wave-front, the image, etc. Indeed, for the image, small pixels are required to get a good representation of the diffraction limited core, but large field of view are also desirable to obtain a good representation of the PSF wings. For example, the AO-PSF of a 30 m telescope in the V-band for a 0.5 asec seeing requires a pixel grid of size at least 2000x2000 in order to preserve the Nyquist sampling.

One simulation method that overcome this explosion in complexity for giant telescopes is the one initially proposed by Rigaut et. al. It is based on a analytical expression of the power spectrum of the residual phase that includes all the first order imperfections of the AO system such as fitting error, aliasing, WFS noise, time delay and anisoplanatism. Then the main computational complexity lies in two fast Fourier transforms that are required to compute the long exposure PSF on the desired pixel grid. This method have the same degree of reality than the other methods mentioned above. Still there is clearly many applications where a slightly reduced accuracy is acceptable, especially in the early stages of a system design, when the basic parameters need to be explored in order to dimension the systems, e.g. compute the Strehl ratio as a function of number of actuators, magnitude of the guide source, etc. In that case, a simulation algorithm able to compute the AO-PSF in minutes rather than hours, days or even weeks is invaluable.

In this paper, we revisit the method from Rigaut et al. It is summarized in section 2 and we also propose an improved bi-dimensional formulation and we apply it to the case of giant telescope. Several examples are given in section 3. As a very important by product of this method, we are able to derive in section 4 a very simple and intuitive relationship between the wings of the AO PSF and the power spectrum of the residual phase: they are basically the same, except that the latter is blurred by the diffraction pattern of the telescope aperture, an effect that is dramatically reduced in the case of giant telescope. Several concluding remarks are presented in section 5.

Further author information: (Send correspondence to L.J.)
L.J.: E-mail: laurent.jolissaint@nrc.ca

2. AN ANALYTICAL MODEL FOR THE PHASE POWER SPECTRUM

2.1. From the phase power spectrum to the AO-PSF

Suppose for the moment that the power spectrum W_φ of the corrected phase is known. We recall that the W_φ is defined by the mean of the phase Fourier transform square norm $W_\varphi(\boldsymbol{f_p}) = \langle|\tilde{\varphi}(\boldsymbol{f_p})|^2\rangle$ where the mean is taken over an infinite number of realizations of the corrected turbulent phase, and $\boldsymbol{f_p}$ is the spatial frequency vector in the pupil plane. From the phase power spectrum, it is possible to calculate the phase structure function (Tatarski, 1961), defined as the mean square difference of the phase between two points separated by a distance vector $\boldsymbol{\rho}$

$$D_\varphi(\boldsymbol{\rho}) = \left\langle \left[\varphi(\boldsymbol{r}+\boldsymbol{\rho}) - \varphi(\boldsymbol{r})\right]^2 \right\rangle = \iint_{\mathbb{R}^2} \left[1 - \cos(2\pi \boldsymbol{f_p}\cdot\boldsymbol{\rho})\right] W_\varphi(\boldsymbol{f_p})\, d^2 f_p \tag{84}$$

The optical transfer function (OTF)[||] of the system composed by the atmosphere, the telescope and the adaptive optics bonette is given by the product of the telescopic OTF (noted T) and a function B_{ao} which is defined as the adaptive optics system OTF. Now, it is known (Conan, 1995) that B_{ao} is given, with a good level of accuracy, by

$$B_{ao}(\boldsymbol{f_i}) = \exp\left[-D_\varphi(\lambda \boldsymbol{f_i})/2\right] \tag{85}$$

where $\boldsymbol{f_i}$ is now the image plane angular frequency vector, which must not be confused with $\boldsymbol{f_p}$, and λ is the imaging wavelength.

To conclude, the AO-PSF can be calculated taking the inverse Fourier transform of the product $T\cdot B_{ao}$, where T will depend only on the telescope design, and B_{ao} on the phase power spectrum, through the relations 84 and 85.

2.2. The phase power spectrum model

We shall give now the principal steps for the derivation of a model of the phase power spectrum. We start with the adaptive optics fundamental equation

$$\varphi_c(\boldsymbol{r},\boldsymbol{\theta},t) = \varphi(\boldsymbol{r},\boldsymbol{\theta},t) - \hat{\varphi}(\boldsymbol{r},\boldsymbol{0},t) \tag{86}$$

where $\varphi_c(\boldsymbol{r},\boldsymbol{\theta},t)$ is the corrected phase at position $\boldsymbol{r}$ in the pupil at time t, looking in a direction $\boldsymbol{\theta}$ relative to the optical axis, and $\hat{\varphi}(\boldsymbol{r},\boldsymbol{0},t)$ is the estimated phase from an on-axis natural guide star (NGS), which can be written

$$\hat{\varphi}(\boldsymbol{r},\boldsymbol{0},t) = \mathcal{R}\left\{\mathcal{M}\left[\frac{1}{\Delta t}\int_{-\Delta t/2}^{+\Delta t/2} \varphi(\boldsymbol{r},\boldsymbol{0},\tau + t - t_d)\, d\tau\right]\right\} + \mathcal{R}\{\nu(\boldsymbol{r},t)\} \tag{87}$$

the integral is over the wave-front sensor (WFS) integration time Δt, $t_d = \Delta t/2 + t_{rc}$ is the mean time delay between the phase measurement and the correction application, where t_{rc} is the time for reading the WFS and calculating the correction. $\mathcal{M}$ is the WFS operator which is assumed linear. For a curvature sensing (CS) WFS, $\mathcal{M}$ corresponds to the measurement of the wave-front curvature, and for a Shack-Hartmann (SH) WFS, it corresponds to the measurement of the wave-front gradient, over the pupil. $\nu(\boldsymbol{r},t)$ is the noise of the WFS measurement. Finally, $\mathcal{R}$ is the reconstructor operator, which gives the estimated phase based on the WFS measurement. The last term of equation 87 is the WFS noise contribution to the reconstructed phase.

In the following, we shall restrict our analysis to the SH-WFS case. The lenslet array is supposedly composed of square lenslets with side length Δ, which correspond also to the actuator pitch on the deformable mirror (DM) as seen in the entrance pupil plane. The DM is considered as a perfect low-pass filter, able to corrected for any perturbation of the phase below the cutting frequency $f_c = 1/2\Delta$. Each lenslet has its associated 4-quadrant detector, consisting of 4 pixels groups on a CCD array. The operators $\mathcal{M}$ and $\mathcal{R}$ are two-dimensional operators, each component being associated with one component of the phase gradient. The measure is written as a convolution of the phase gradient with the rectangular function, associated with the mean of the phase slope over each lenslet, times the sampling function, associated with the sampling of the later quantity over the lenslet array

$$\mathcal{M}\left[\varphi(\boldsymbol{r},t)\right] = \left[\nabla\varphi(\boldsymbol{r},t) * \Pi(\boldsymbol{r}/\Delta)\right]\cdot \underline{\mathrm{III}}(\boldsymbol{r}/\Delta) \tag{88}$$

The reconstructor is simply given by the inverse of $\mathcal{M}$, but without the sampling term $\underline{\mathrm{III}}$.

Now, let us define $\mathcal{B}$ as any infinite orthogonal basis of continuous, integrable functions defined in the pupil, and let us write $\mathcal{E}$ as the vectorial space associated with this basis. Afterwards, let us define $\mathcal{E}_{||}$ as the sub-space of $\mathcal{E}$ associated

[||]which is defined by the bi-dimensional Fourier transform of the system PSF with the eigen functions of the DM, and $\mathcal{E}_\perp$ with its orthogonal space. As we consider the DM as a perfect spatial filter below the frequency f_c, $\mathcal{E}_{||}$ is associated with all the functions containing spatial frequencies below f_c, and $\mathcal{E}_\perp$ with all the other functions. Now, we split the incoming phase in the pupil over this two sub-spaces :

$$\varphi(\boldsymbol{r},\boldsymbol{\theta},t) = \varphi_{||}(\boldsymbol{r},\boldsymbol{\theta},t) + \varphi_\perp(\boldsymbol{r},\boldsymbol{\theta},t) \tag{89}$$

therefore, $\varphi_{||}$ is associated with the components of the phase that can be corrected by the DM, or low frequency component, and $\varphi_\perp$ with the component that the DM cannot correct, or high frequency component. Note that we shall suppose thereafter that the DM is able to correct the phase independently of the direction. As a consequence, the low frequency component will be limited to the *circular* domain $|\boldsymbol{f_p}| \leq f_c$.

At this point, we have everything in hand to construct the phase spatial power spectrum. Nevertheless, we shall not give the detailed calculation here, first because it is partly given in Rigaut et al., and secondly because space is restricted. Rather, we shall explain the approach and give the final result.

Using equations 86, 87 and 89 allows us to decompose the compensated phase into the five classical terms,

$$\begin{aligned}
\varphi_c(\boldsymbol{r},\boldsymbol{\theta},t) &= \varphi_\perp(\boldsymbol{r},\boldsymbol{\theta},t) + \Big[\varphi_{||}(\boldsymbol{r},\boldsymbol{\theta},t) - \varphi_{||}(\boldsymbol{r},\boldsymbol{0},t)\Big]_{\text{aniso}} \\
&+ \left[\varphi_{||}(\boldsymbol{r},\boldsymbol{0},t) - \mathcal{R}\left\{\mathcal{M}\left[\frac{1}{\Delta t}\int_{-\Delta t/2}^{+\Delta t/2} \varphi_{||}(\boldsymbol{r},\boldsymbol{0},\tau+t-t_d)\,d\tau\right]\right\}\right]_{\text{servo-lag}} \\
&- \mathcal{R}\left\{\mathcal{M}\left[\frac{1}{\Delta t}\int_{-\Delta t/2}^{+\Delta t/2} \varphi_\perp(\boldsymbol{r},\boldsymbol{0},\tau+t-t_d)\,d\tau\right]\right\}_{\text{alias}} - \mathcal{R}\{\nu(\boldsymbol{r},t)\}_{\text{noise}}
\end{aligned} \tag{90}$$

$\varphi_\perp$ is the high frequency component; the anisoplanatism component comes from the fact that the system tries to correct the phase in the direction $\boldsymbol{\theta}$ based on a phase measurement on axis; the servo-lag component is related to the temporal averaging of the phase during the measurement, plus the unavoidable delay between the later and the application of the correction; the aliasing component is simply related to the fact that the phase fluctuations at spatial frequencies higher than f_c are seen, by the WFS, as fluctuations in the 0 to f_c domain; finally, the noise component is related to the WFS noise (photon and read noise). Note that while the first term is obviously defined in the high frequency domain, the others are defined only for the low frequency domain $f_p < f_c$.

Taking the Fourier Transform of equation 90, and making the assumption that the different terms are not correlated, we can write the compensated phase power spectrum as the sum of the five terms power spectrums

$$W_\varphi^c(\boldsymbol{f_p},\boldsymbol{\theta}) = W_\varphi^{hf}(\boldsymbol{f_p}) + W_\varphi^{an}(\boldsymbol{f_p},\boldsymbol{\theta}) + W_\varphi^{sl}(\boldsymbol{f_p}) + W_\varphi^{al}(\boldsymbol{f_p}) + W_\varphi^{ns}(\boldsymbol{f_p}) \tag{91}$$

the expressions of each we are going to give below.

Model of the turbulent atmosphere

We shall suppose that the turbulent atmosphere is composed of N independent thin turbulent layers at altitudes h_i, each with its proper r_0^i value, and that each of these layers is blowed across the optical beam at a velocity $\boldsymbol{v_i}$. We shall also suppose that the turbulent regime is Kolmogorov fully developed, i.e. without any outer or inner scale. Then, the power spectrum of the uncorrected phase is given by $W_\varphi^{atm}(\boldsymbol{f_p}) = 0.0229\, r_0^{-5/3}\, f_p^{-11/3}$.

High frequency spectrum

This term is simply given by the turbulent phase power spectrum above the cutting frequency f_c, i.e.

$$W_\varphi^{hf}(\boldsymbol{f_p}) = W_\varphi^{atm}(\boldsymbol{f_p}) \;\text{ for } |\boldsymbol{f_p}| > f_c \;,\; 0 \;\text{ otherwise} \tag{92}$$

Anisoplanatism spectrum

Writing the total phase in the pupil as the sum of the phase delay in each layers $\varphi(\boldsymbol{r},\boldsymbol{\theta},t) = \sum_{i=1}^N \varphi_i(\boldsymbol{r} + h_i\boldsymbol{\theta},\boldsymbol{0},t)$, we found for the contribution of the anisoplanatism term

$$W_\varphi^{an}(\boldsymbol{f_p}) = 0.0458\, f_p^{-11/3} \sum_{i=1}^N r_{0,i}^{-5/3} \left[1 - \cos\left(2\pi h_i \boldsymbol{f_p}\cdot\boldsymbol{\theta}\right)\right] \;\text{ for }\; |\boldsymbol{f_p}| < f_c \tag{93}$$

Servo-lag spectrum

Using firstly the fact that in each layer $\varphi_i(\boldsymbol{r}, \tau + t - t_d) = \varphi_i(\boldsymbol{r} - (\tau - t_d)\boldsymbol{v_i}, t)$, secondly the fact that we suppose the operators $\mathcal{M}$ and $\mathcal{R}$ linear so as they can commute with the sum over the integration time, and thirdly that the reconstructor is perfectly able to reconstruct the low frequency phase component based on a perfect measurement, i.e. writing $\mathcal{R}\{\mathcal{M}[\varphi_{||}]\} = \varphi_{||}$, we found, where $\mathrm{sinc}(x) \equiv \sin(\pi x)/\pi x$,

$$W_\varphi^{sl}(\boldsymbol{f_p}) = 0.0229\, f_p^{-11/3} \sum_{i=1}^{N} r_{0,i}^{-5/3} \left[1 - 2\cos\left(2\pi t_d \boldsymbol{f_p}\cdot\boldsymbol{v_i}\right) \mathrm{sinc}(\Delta t \boldsymbol{f_p}\cdot\boldsymbol{v_i}) + \mathrm{sinc}^2(\Delta t \boldsymbol{f_p}\cdot\boldsymbol{v_i})\right] \quad \text{for } |\boldsymbol{f_p}| < f_c \tag{94}$$

Aliasing spectrum

At this point of our work, we have momentary decided to made a crude approximation for the aliased spectrum. First, we have ignored the contribution of the integration time, and second, we have made the assumption that the bi-dimensional spectrum can be approximated at each direction in the frequency plane by the value of the mono-dimensional case, which is given in the paper of Rigaut et al. We found then

$$W_\varphi^{al}(\boldsymbol{f_p}) = 0.0229 \sum_{i=1}^{N} \sum_{n=1}^{\infty} r_{0,i}^{-5/3} \left[(f_p + 2nf_c)^{-11/3} + (f_p - 2nf_c)^{-11/3})\right] \quad \text{for } |\boldsymbol{f_p}| < f_c \tag{95}$$

it is clear that this expression will not give accurate results when used with long integration time, but the effect of the later is of second order relative to the effect of the aliasing of the high frequency component of the phase spectrum into the low frequency domain. We hope to give a more complete expression in a future version of this work.

Noise spectrum

The power spectrum of the noise is simply given by the product of the reconstructor Fourier transform square norm and the power spectrum of the noise on the angle of arrival measurement over each lenslet, i.e. $W_\varphi^{ns} = \left|\tilde{\mathcal{R}}\right|^2 \left\langle |\tilde{\nu}|^2 \right\rangle$. It can be shown based on Rigaut et al. paper that $\left|\tilde{\mathcal{R}}\right|^2$ writes

$$\left|\tilde{\mathcal{R}}\right|^2 = \left[f_p^2\, \mathrm{sinc}^2(\Delta f_{p,x})\, \mathrm{sinc}^2(\Delta f_{p,y})\right]^{-1} \tag{96}$$

$\left\langle |\tilde{\nu}|^2 \right\rangle$ is supposed to be a white spectrum inside the low frequency space, then is related to the variance of the measurement by $\langle |\tilde{\nu}|^2 \rangle = \pi\, f_c^2\, \sigma_{nea}^2$, where σ_{nea}^2 is the square of the Noise Equivalent Angle, which can be found, for a 4-quadrant detector, in Tyler and Fried (1982), for example, and is dependent on the full width at half maximum of the lenslet image and of the total signal on noise ratio of the total photon fluxes in the detector. We shall not give these relations here.

3. SOME TEST RESULTS OF THE SIMULATED AO-PSF

To test the behavior of the simulated AO-PSF, we have choosen to study the evolution of the Strehl ratio versus some of the main parameters of an usual AO system, for a moderate size telescope.

The parameters of the simulated AO-system are : telescope diameter 3.6 m, wavelength 1.6 μm, seeing 0.5", Mauna Kea turbulence vertical profiles, SH-WFS with 5 e/px read noise, magnitude 14 G0 type NGS on axis, actuator pitch equal to the r_0 at 1.6 μm, WFS integration time equal to the characteristic time life of the speckles at 1.6 μm, pure delay 0.1 ms.

3.1. Strehl ratio and number of actuators

With all the others parameters fixed, we have calculated the AO-PSF for various values of the number of actuators over the telescope diameter. We find, as expected, that there exists an optimum number of actuators for a given NGS magnitude (figure 1, left). Indeed, starting from few actuators, it is clear that increasing their number will increase the quality of the correction. But after the Strehl reaches an optimum value, it starts to decrease, due to the decrease of the number photon per lenslet (flux dilution), whose size is defined by the actuator pitch. Here, it is interesting to see that this optimal value is close to the ratio $D/r_0(\lambda)$, a rule-of-thumb value to get a good correction of the phase.

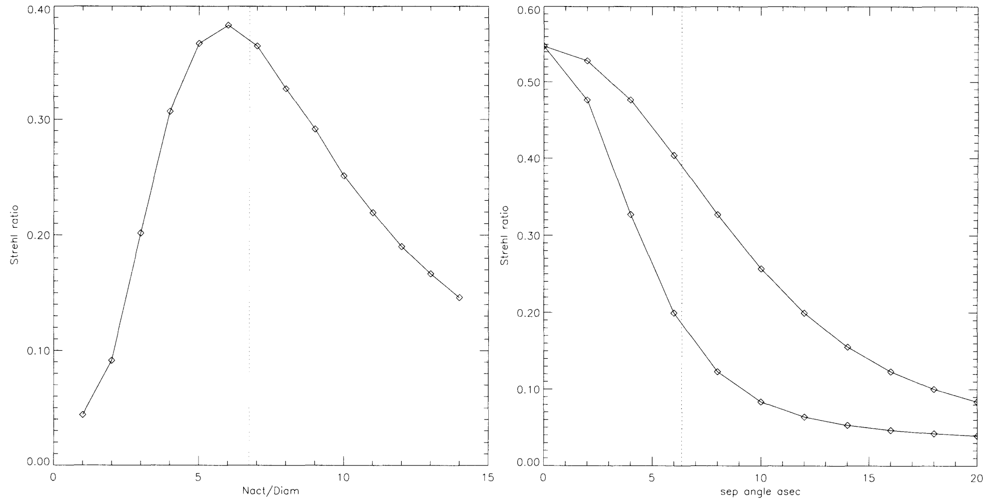

Figure 1. Left figure, Strehl ratio versus the number of actuators across the pupil diameter. The vertical line shows the $D/r_0 = 6.7$ value for the simulation. Right figure, Strehl ratio and off-axis angle position of the NGS. Upper curve is for a vertical profile of C_N^2 equal to the mean Mauna Kea profile, lower curve is for the same profile, but with the altitudes associated with the layers increased by a factor of two. Vertical line shows the value of the isoplanatic angle, following the equation given below.

3.2. Strehl ratio, anisoplanatism and layers mean altitude

Here, we have set the number of actuators to the D/r_0 value, and we have progressively moved the NGS away from the optical axis, while imaging an on-axis point source. In a second experiment, we have done the same thing but increasing the altitude of the turbulence layers by a factor two (figure 1, right). We find a decrease of the Strehl with the NGS off-axis position which is consistent with the value of the anisoplanatism angle defined by the usual expression $0.314\, r_0/\langle h \rangle$ where $\langle h \rangle$ is the mean altitude of the turbulent layers (Beckers, 1993). Beside, when we increase the altitude of all the layers by a given factor, we see that the angle for the Strehl to reach a certain value is decrease by the same factor, here a factor of two.

3.3. Strehl ratio and NGS magnitude

Here, with the NGS on-axis, we examine the effect of increasing the NGS magnitude, i.e. increasing the WFS noise. The decrease of the Strehl show a classical behavior, i.e. an almost constant value below a certain limit, and a rapid decrease to the non-AO Strehl above this limit, which is, in our simulation, somewhere around the 15th magnitude (figure 2, left).

3.4. Strehl ratio, integration time and WFS read noise

As a last example, we have choosen to examine the effect of the integration time, first without WFS read noise, then with a read noise of 5 e/px (figure 2, right). We find, as expected, that there exists an optimum value of the integration time, which results from the balancing of the effect of the servo-lag and the effect of the noise. Here, it is interesting to see that the optimal value is near the typical time-life of the speckles, which is given by $0.314\, r_0/\langle V \rangle$ where $\langle V \rangle$ is the mean velocity of the turbulent layers (Beckers, 1993). Beside, we can see that increasing the WFS read noise has a strong effect on the Strehl, but only for the shortest integration times where the WFS SNR is significantly degraded. At the lowest value of Δt, the effect of the noise on the Strehl ratio is small. The main contributor then is the servo-lag error, which is independent of the read noise.

4. THE CORRECTED PHASE POWER SPECTRUM AND THE AO-PSF WINGS

We present now the second part of our work, related to the interpretation of the effect of the phase correction on the AO-PSF.

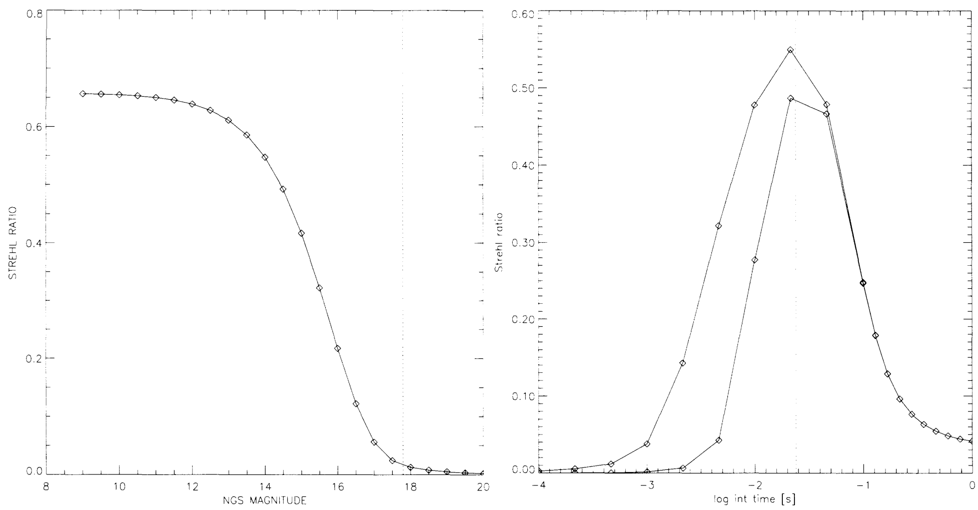

Figure 2. Left figure, Strehl ratio versus NGS magnitude. The vertical line shows where the WFS SNR is less than 2. Right figure, Strehl ratio and integration time. The vertical line shows the value of the speckles life time.

The point spread function S of any optical system is given by the square modulus of the Fourier transform of the phasor $U_p(\boldsymbol{r}) = \exp[i\varphi(\boldsymbol{r})]$ in the optical system pupil:

$$S(\boldsymbol{x}) \sim \left|\tilde{U}_p\right|^2(\boldsymbol{f_p}) = \left|\iint\limits_{P} e^{i\varphi(\boldsymbol{r})}\, e^{-i2\pi \boldsymbol{f_p}\cdot\boldsymbol{r}}\, d^2\boldsymbol{r}\right|^2 \tag{97}$$

The position $\boldsymbol{x}$ in the focal plane is related to the pupil spatial frequency $\boldsymbol{f_p}$ by $\boldsymbol{x} = F\lambda\boldsymbol{f_p}$, where F is the focal length. In other terms, the PSF at an angular position $\boldsymbol{\alpha} = \boldsymbol{x}/F$ can be seen as the power spectrum of the phasor at the pupil frequency $\boldsymbol{f_p} = \boldsymbol{\alpha}/\lambda$. This interpretation is known as the *angular spectrum interpretation* (Goodman, 1996).

Now, let us make a useful approximation. Suppose the AO is effective enough so as the residual phase variance is small, e.g. less than $1\,rad^2$. In this case, the phasor can be well approximated by $\exp(i\varphi) \approx 1 + i\varphi - \varphi^2/2$. Using this approximation, it can be shown that the instantaneous PSF may be approximated by:

$$S \sim \left|\tilde{P}\right|^2 + 2\,\mathrm{Im}\Big\{\tilde{P}\cdot\big(\overline{\tilde{P}*\tilde{\varphi}}\big)\Big\} - \mathrm{Re}\Big\{\tilde{P}\cdot\big(\overline{\tilde{P}*\tilde{\varphi}*\tilde{\varphi}}\big)\Big\} + \left|\tilde{P}*\tilde{\varphi}\right|^2 \tag{98}$$

where $\tilde{P}$ is the Fourier transform of the pupil transmittance (1 in the pupil, 0 outside), and $\tilde{\varphi}$ is the Fourier transform of the instantaneous phase. Note that it is necessary to keep the second order term in the phasor approximation above to take into account all the 4 order terms in the development of equation 98. Now, the long exposure PSF is defined by the temporal mean of S. Taking into account that $\langle\tilde{\varphi}\rangle = 0$ and that the pupil transmittance is even for usual telescopes, we have:

$$\langle S\rangle \sim \left|\tilde{P}\right|^2 - \tilde{P}\cdot\left(\tilde{P}*\mathrm{Re}\{\langle\tilde{\varphi}*\tilde{\varphi}\rangle\}\right) + \left\langle\left|\tilde{P}*\tilde{\varphi}\right|^2\right\rangle \tag{99}$$

We consider now the case of an infinite telescope, in order to get the contribution of the corrugated phase only. The pupil function is then replaced by a Dirac distribution δ. As $\delta\cdot\mathrm{Re}\{\langle\tilde{\varphi}*\tilde{\varphi}\rangle\}$ has non zero values only at $\boldsymbol{f_p}=0$, we find that this term is equal to $\delta\cdot\sigma_\varphi^2$, where σ_φ^2 is the residual phase variance. Beside, the last term of equation 99 turns to $\langle|\tilde{\varphi}|^2\rangle$, which is nothing else than the **power spectrum of the residual phase** W_φ that we have calculated in the first part on this paper. Then, recalling the angular spectrum interpretation, we have:

$$\langle S_\delta\rangle(\boldsymbol{\alpha}) \sim \left[\delta^2(\boldsymbol{\alpha}/\lambda) - \delta(\boldsymbol{\alpha}/\lambda)\cdot\sigma_\varphi^2\right]_{\mathrm{core}} + W_\varphi(\boldsymbol{\alpha}/\lambda)_{\mathrm{wings}} \tag{100}$$

where the AO-PSF is now separated into a Dirac's core, and phase power spectrum wings. In other words, we assert here that the wings of the AO-PSF for a (very) large telescope at an angular position $\boldsymbol{\alpha}$, is given, in a first approximation, by the power spectrum of the residual phase at the pupil frequency $\boldsymbol{f_p} = \boldsymbol{\alpha}/\lambda$.

In figure 3, we give an example of a phase power spectrum calculated from equations 91 to 96, compared to the infinite telescope case and a finite (20 m) telescope case AO-PSF. The parameters for the simulation are : Mauna Kea like turbulence profiles, magnitude 0 NGS, $\lambda = 1.65\,\mu m$, 1 actuator per $r_0(1.65\,\mu m)$, i.e. 22 actuators over the 20 m diameter.

Clearly, the approximation is very good for assessing the AO-PSF wings, even for the finite size telescope. Beside, we see that the transition in the spectrum between the low to the high frequency domain, which is given by the cut-off frequency of the DM $f_c = 1/2\Delta$, allows us to predict an angular transition from the diffraction limited core to the atmospheric residual halo at a value $\alpha_t = \lambda f_c = \lambda/2\Delta$. We believe that such a strong transition has not be seen on existing AO systems simply because it was buried in the diffraction pattern of the telescope aperture. Indeed, for this transition to be seen, α_t must be larger than the radius of the first diffraction rings, i.e. $D/\Delta \gg 5$. This may be the case for the AO systems on the new generation 10 m class telescopes AO systems, but probably not for the first generation AO systems (PUEO, ADONIS, ...).

Thanks to this approach, we are now able to predict the effect of any kind of phase correction on the AO-PSF**. In particular, since the anisoplanatism, noise and servo-lag contribute to the low frequency part of the spectrum, we can predict that all that affect these components will affect the central part of the AO-PSF. In contrast, the WFS aliasing error will affect more the external parts of the AO-PSF, but always inside the $\alpha < \alpha_t$ region.

5. CONCLUSIONS

We have revisited the method proposed by Rigaut et al. (1998) and implemented it with a more accurate bi-dimensional formulation. The major advantage of this approach is to enable the computation of the AO corrected long exposure PSF, without requiring a huge amounts of computation and still preserving a good accuracy. This advantage becomes critical for the next generation of giant telescopes, where the computation can be performed in a few minutes instead of hours or days. We believe this tool is very useful for a first assessment of the performance of an AO system, as well as for the quick generation of AO corrected PSF, e.g. for simulating science images. Tests show that the model has a consistent behavior. Some improvements are nevertheless possible, the most important could be a more accurate treatment on the aliasing; it should be possible to make a curvature sensing version of this model, too. Finally, it will be useful to include more than one DM and WFS in the spectrum, making this model able to predict the MCAO AO-PSF as well.

We have also shown that for giant telescopes and a good level of AO correction, the shape of the PSF is given by the power spectrum of the residual phase. This interpretation is a very powerful tool to understand and predict the effect of the observing conditions and of the characteristics of the AO system in the image plane.

ACKNOWLEDGMENTS

We would like to thank François Rigaut for providing us with a copy of its simulation code, which served as the basis for our own code. We are also very grateful to the Swiss National Fund for making this research work possible by providing a grant for Laurent Jolissaint.

REFERENCES

Rigaut F., Veran J.P., and Lai O., "An analytical model for Shack-Hartmann based adaptive optics systems," *Proc. SPIE* **3353**, pp. 1038–1048, 1998.

Tatarski V.I, *Wave propagation in a turbulent medium, translated by R.A.Silverman*, Dover Publications, New York, 1961.

Conan J.M., *Etude de la correction partielle en optique adaptative*, ONERA, Paris, 1995.

Tyler G. A. and Fried D. L., "Image-position error associated with a quadrant detector," *Journal of the Optical Society of America* **72**, 1982.

Goodman J.W., *Introduction to Fourier optics*, 2nd Ed., McGraw Hill, 1996.

Beckers J. M., "Adaptive optics for astronomy, principles, performances, applications," *Annual Review of Astronomy & Astrophysics* **31**, 1993.

**it must to be noted, in fact, that this approximation is independent of the model developed above for the phase power spectrum, and can be used with any other method able to give a numerical or theoretical value of the phase spectrum

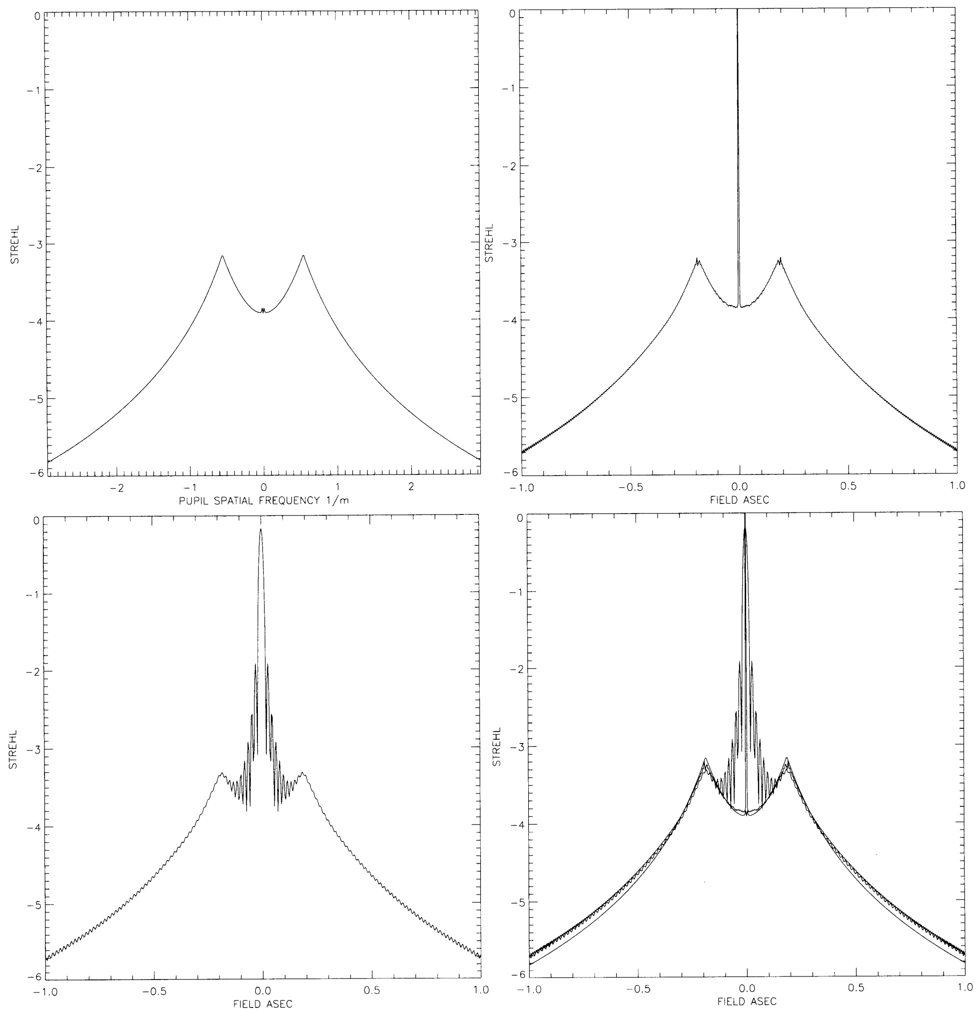

Figure 3. Upper left, phase power spectrum. What we see is essentially the high frequency part (above f_c), and a low frequency part dominated by the aliasing. Upper right, AO-PSF for an infinite telescope, associated with the later phase power spectrum. Lower left, same, but for a 20 m telescope. Lower right, super-imposition of the three figures.